Journal of Digital Imaging (2023) 36:2313–2321
https://doi.org/10.1007/s10278-023-00864-3

Effect of Gaussian Smoothing Filter Size for CT-Based Attenuation Correction on Quantitative Assessment of Bone SPECT/CT: A Phantom Study

Yoya Tomita[1] · **Yasutaka Ichikawa**[2] · **Kengo Hashizume**[1] · **Hajime Sakuma**[2]

Received: 4 March 2023 / Revised: 15 May 2023 / Accepted: 30 May 2023 / Published online: 15 June 2023

Abstract

This study aims to determine the effect of Gaussian filter size for CT-based attenuation correction (CTAC) on the quantitative assessment of bone SPECT. An experiment was performed using a cylindrical phantom containing six rods, of which one was filled with water and five were filled with various concentrations of K_2HPO_4 solution (120–960 mg/cm^3) to simulate different bone densities. ^{99m}Tc-solution of 207 kBq/ml was also included within the rods. SPECT data were acquired at 120 views for 30 s/view. CT for attenuation correction were obtained at 120 kVp and 100 mA. Sixteen different CTAC maps processed with different Gaussian filter sizes (ranging from 0 to 30 mm in 2 mm increments) were generated. SPECT images were reconstructed for each of the 16 CTAC maps. Attenuation coefficients and radioactivity concentrations in the rods were compared with those in the water-filled rod without K_2HPO_4 solution as a reference. Gaussian filter sizes below 14–16 mm resulted in an overestimation of radioactivity concentrations for rods with high concentrations of K_2HPO_4 ($\geq$ 666 mg/cm^3). The overestimation of radioactivity concentration measurement was 3.8% and 5.5% for 666 mg/cm^3 and 960 mg/cm^3 K_2HPO_4 solutions, respectively. The difference in radioactivity concentration between the water rod and the K_2HPO_4 rods was minimal at 18–22 mm. The use of Gaussian filter sizes smaller than 14–16 mm caused an overestimation of radioactivity concentration in regions of high CT values. Setting the Gaussian filter size to 18–22 mm enables radioactivity concentration to be measured with the least influence on bone density.

Keywords Gaussian filter · CT-based attenuation correction · Attenuation coefficient · Bone quantitative single photon emission computed tomography/computed tomography (SPECT/CT)

Background

Bone scintigraphy using radioactive tracers is widely used in routine clinical practice to evaluate bone metabolic abnormalities associated with malignant bone disease. The advent of scanners that integrate single-photon emission computed tomography (SPECT) and computed tomography (CT) has greatly improved the diagnostic performance of bone scintigraphy for detecting bone metastasis compared to conventional two-dimensional imaging [1, 2]. SPECT/CT enables the acquisition of three-dimensional data and the creation of the attenuation correction maps that are necessary to accurately quantify tissue uptake of radionuclides. Quantitative SPECT/CT analysis techniques have made it possible in determining standardized uptake values (SUVs) of bone tissue [3–5]. Recent studies have shown that quantitative SPECT evaluation of bone scintigraphy using SUV thresholds is useful for differentiating between bone metastases and benign lesions [6–9]. According to a study that used ^{99m}Tc-2,3-dicarboxy propane1,1-diphosphonate (DPD) SPECT/CT to evaluate 171 sites of osseous metastases from prostate cancer [8], diagnostic performance for identifying bone metastases in the pelvic bone and spine was highest using a maximum SUV (SUV_{max}) cutoff value of 19.5.

CT-based attenuation correction (CTAC) is required to be performed for quantitative evaluation of bone SPECT/

✉ Yasutaka Ichikawa
yasutaka@med.mie-u.ac.jp

Yoya Tomita
kurochibi55@med.mie-u.ac.jp

Kengo Hashizume
hszmcrad@med.mie-u.ac.jp

Hajime Sakuma
sakuma@med.mie-u.ac.jp

[1] Central Division of Radiology, Mie University Hospital, 2-174 Edobashi, Tsu, Mie 514-8507, Japan

[2] Department of Radiology, Mie University Hospital, 2-174 Edobashi, Tsu, Mie 514-8507, Japan

CT [10]. In the CTAC process, the CT images are converted into attenuation coefficient maps corresponding to the photon energies of the radionuclides used in the SPECT examination, and the resulting maps are then smoothed by a Gaussian filter. The smoothing process of the CTAC map with a Gaussian filter is needed to reduce artifacts caused by the different resolutions of the SPECT and CT images [11, 12]. Since the size of the Gaussian filter can affect the attenuation coefficient, it may also affect the accuracy of the SPECT quantitative assessment. Determining the impact of Gaussian filter size on the quantitative assessment of SPECT is considered important for the future widespread use of this nuclear medicine technique in clinical practice. However, until now, there have been no reports evaluating the influence of the size of the Gaussian filter used for smoothing the CTAC map in SPECT quantitative evaluation. The purpose of this phantom study is to evaluate the effect of Gaussian filter size on attenuation coefficient and absolute activity concentration in bone SPECT/CT.

Material and Methods

Phantom Preparation

A cylindrical phantom with both an inner diameter and height of 20 cm (JSP type, Kyoto Kagaku Co., Ltd, Kyoto, Japan) was used in this study (Fig. 1A). The phantom contained six rods, each 30 mm in diameter (Fig. 1B a–f). The background part and central rod were filled with 17 kBq/mL of ^{99m}Tc-pertechnetate solution with an energy peak of 140.5 keV for the emitted photons. All six rods contained ^{99m}Tc-pertechnetate solution at the same radioactivity concentration (207 kBq/mL), with a rod-to-background ratio of 12.2. One of the rods was filled with water and five were filled with K_2HPO_4 solution of various concentrations (120, 275, 450, 666, and 960 mg/cm^3) to simulate different bone densities [13–16]. The K_2HPO_4 concentrations were set based on the CT densities of normal and osteosclerotic lesions [17–19].

Image Acquisition and Reconstruction

SPECT/CT imaging of the phantom was performed by a hybrid Discovery NM/CT670 (General Electric Medical Systems, Milwaukee, WI) with dual-head NaI(Tl) detectors equipped with low-energy high-resolution collimators. SPECT imaging was performed with two rotations of 22 cm in continuous acquisition mode. The parameters included a symmetric width of 10% for the main window centered at the 140.5 keV photopeak and a symmetric width of 5% for the scatter window centered at 120 keV, 128 × 128 matrix, H-mode with a total of 120 projections (60 steps with 360°/head and 1 repeat) with a dwell time of 30 s/view. CT imaging for attenuation correction was performed with a tube voltage of 120 kVp. The tube current and rotation time were fixed to 100 mA and 0.5 s, respectively. The CT images were reconstructed with 1.25 mm of slice thickness, standard

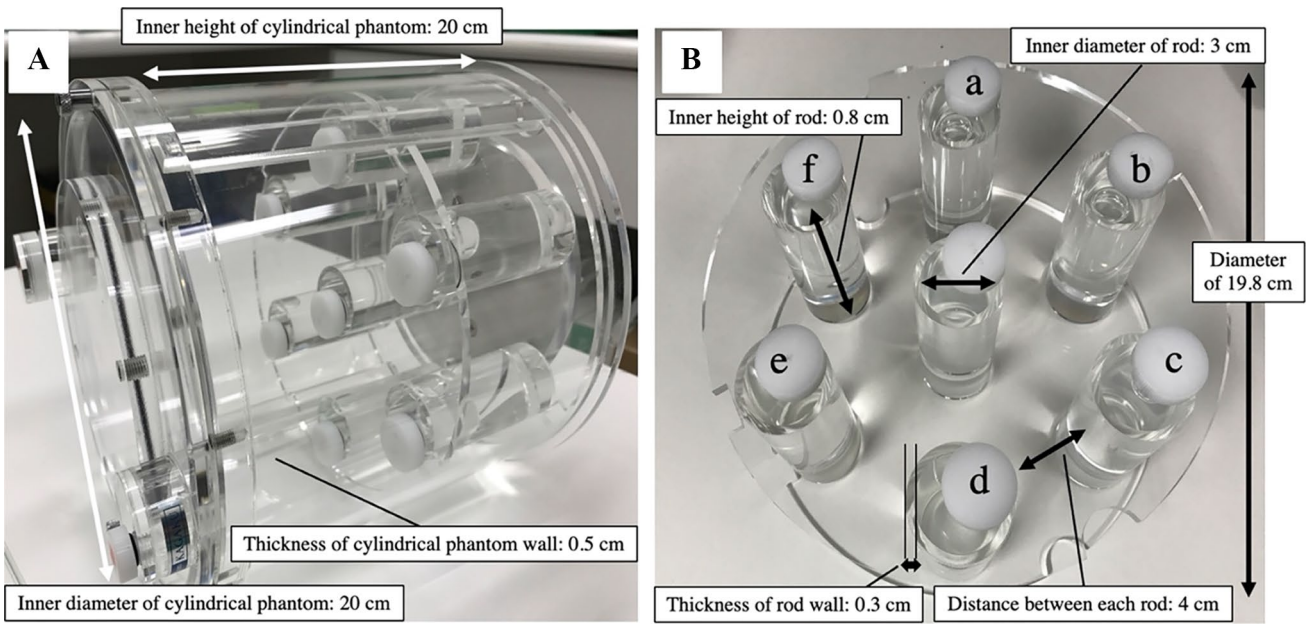

Fig. 1 Photograph of the cylindrical phantom (**A**) showing the six rods of 30-mm diameter used in this study (**B**). One rod was filled with water (a) and five rods were filled with K_2HPO_4 solution of concentrations 120 (b), 275 (c), 450 (d), 666 (e), and 960 (f) mg/cm^3 to simulate different bone densities

kernel, 50 cm of field of view, and 512 × 512 matrix size. For further image processing, the SPECT data and CT images were transferred to a commercially available workstation (Xeleris Functional Imaging Workstation (Xeleris 3.1, General Electric Medical Systems, Milwaukee, WI). The CT data were downsampled to the same matrix size as the SPECT data (128 × 128) and converted to an CTAC map using a bilinear method. The CTAC maps were smoothed with a Gaussian filter of size (full width at half maximum) ranging from 2 to 30 mm in 2 mm increments, and also without a Gaussian filter. Therefore, 16 different CTAC maps were generated. Attenuation correction was then performed for the SPECT images using each of the 16 different CTAC maps. The SPECT data were reconstructed using three-dimensional iterative ordered subset expectation maximization (OSEM, 10 subsets and 2 iterations) with CTAC, scatter correction, and resolution recovery. A Butterworth post-filter was used with a power of 10 and cutoff frequency of 0.5 cycles/cm. The SPECT images were reconstructed with a slice thickness of 2.21 mm. Quantitative SPECT images were then reconstructed using the system sensitivity, with the count values converted to radioactivity concentration for each pixel.

Image Analysis

Image analysis was performed on a Xeleris Functional Imaging Workstation (General Electric Medical Systems). The mean CT number and attenuation coefficient in each rod were measured by placing circular regions of interest (ROIs) with 24 mm in diameter within the rods on the six different cross-sections of the central part of the rods on CT images and CTAC maps, respectively. Circular ROIs were placed in the six cross-sections identical to the CT images and CTAC maps, and the maximum radioactivity concentration in the central part of each rod was measured. The maximum radioactivity concentration in the background region was measured in each SPECT image by placing a circular ROI with a diameter of 60 mm in the central 6 slices of the phantom. In addition, lines were drawn through the center of each rod in the middle slice of SPECT images, and line profile curves were drawn to evaluate the distribution of radioactivity within the rods.

Statistical Analysis

Statistical analysis was performed using JMP version 10.0 (SAS Institute Inc.). Data are presented as the median and interquartile range. p values < 0.05 were considered statistically significant. The attenuation coefficients and radioactivity concentration in the rods filled with different concentrations of K_2HPO_4 solution were respectively analyzed by steel nonparametric method, using the attenuation coefficients in the rods without K_2HPO_4 solution as the reference. We then calculated the difference in radioactivity concentration between rods with and without K_2HPO_4 solution for each Gaussian filter size, using the following formula:

((Radioactivity concentration with K_2HPO_4 solution
− radioactivity concentration without K_2HPO_4 solution)
/radioactivity concentration without K_2HPO_4 solution) × 100 (%).

Results

CT Density and Attenuation Coefficient

The CT image obtained at 120 kVp and the attenuation coefficient maps are shown in Fig. 2, and Table 1 lists the CT density measurements in the rods. The relation between Gaussian filter size and the measured attenuation coefficients is presented in Fig. 3. In rods with higher K_2HPO_4 concentrations, the attenuation coefficients were highest with the smallest Gaussian filter sizes. For example, in the rod with 960 mg/cm^3 of K_2HPO_4 solution, the attenuation coefficients with no Gaussian filter and with Gaussian filters of size 10, 20, and 30 mm were 0.243, 0.236, 0.219, and 0.199 cm^{-1}, respectively. In contrast, the attenuation coefficient was relatively constant for the rod without K_2HPO_4 solution, regardless of Gaussian filter size. Attenuation coefficients were significantly higher for rods at every K_2HPO_4 concentration than for rods without K_2HPO_4 solution at all Gaussian filter sizes ($p < 0.05$) (Fig. 3).

Radioactivity Concentration in the Rods

Figure 4 shows SPECT images with attenuation correction using the smoothed CTAC maps with different Gaussian filter sizes. Visually, the radioactivity concentration in rods with higher K_2HPO_4 concentrations appeared higher than that in the rod without K_2HPO_4 solution when the Gaussian filter size was small. When the Gaussian filter size was larger than 20 mm, however, the radioactivity concentration in the rods was almost constant for all K_2HPO_4 concentrations. The relation between radioactivity concentration in the rods and Gaussian filter size is presented in Fig. 5. The maximum measured radioactivity concentrations in the rod without K_2HPO_4 solution on SPECT images were ranging from 243.1 to 249.6 kBq/ml. These measured activity concentrations showed an overestimation of 17.4–20.6% from true radioactivity (207 kBq/ml). The maximum measured radioactivity concentration of the background was a median of 16.3 kBq/ml. When Gaussian filter size was less than 14–16 mm, the

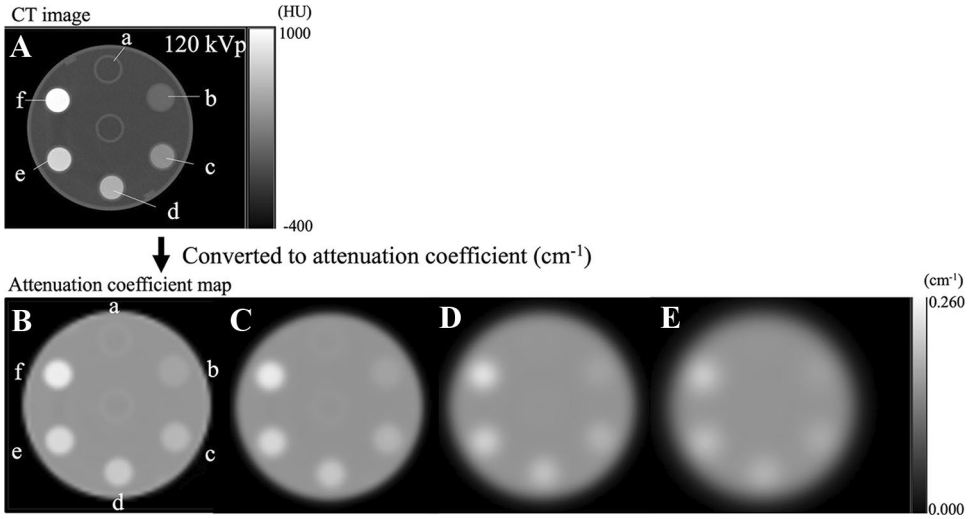

Fig. 2 CT image of the phantom obtained at 120 kVp (**A**) and CT-based attenuation coefficient maps smoothed with no filter (**B**) and with Gaussian filter sizes of 10 (**C**), 20 (**D**), and 30 (**E**) mm. Rod (a) was filled with water, and rods (b–e) were filled with K_2HPO_4 solution of concentrations 120 (b), 275 (c), 450 (d), 666 (e), and 960 (f) mg/cm^3 to simulate different bone densities

Table 1 CT density of the rods according to K_2HPO_4 concentration

K_2HPO_4 concentration (mg/cm^3)	CT number (HU)
None	5.0 (4.3–5.0)
120	175.0 (175.0–175.0)
275	385.0 (385.0–385.8)
450	576.0 (576.0–576.8)
666	761.5 (761.0–762.0)
960	996.0 (996.0–996.0)

Data are presented as the median (interquartile range)

measured radioactivity concentration in rods with 666 and 960 mg/cm^3 of K_2HPO_4 solution showed significant overestimation ($p < 0.05$) compared to that in the rod without K_2HPO_4 solution. For example, when the Gaussian filter size was 10 mm, there was a significant overestimation of radioactivity concentration measurement of 3.0% ($p = 0.022$) for K_2HPO_4 solution of 666 mg/cm^3 and 4.5% ($p = 0.022$) for K_2HPO_4 solution of 960 mg/cm^3. When the Gaussian filter size was 4 mm, there was a significant overestimation of radioactivity concentration measurement of 3.8% ($p = 0.022$) for K_2HPO_4 solution of 666 mg/cm^3 and 5.5% ($p = 0.022$) for K_2HPO_4 solution of 960 mg/cm^3. The smallest mean difference in radioactivity concentration between rods with and without K_2HPO_4 solution was for Gaussian filter size of 18–22 mm, with an error within 1.0% (Fig. 6). The line profile curves through the rod center on the SPECT images are shown in Fig. 7. In all rods, the maximum radioactivity concentration was

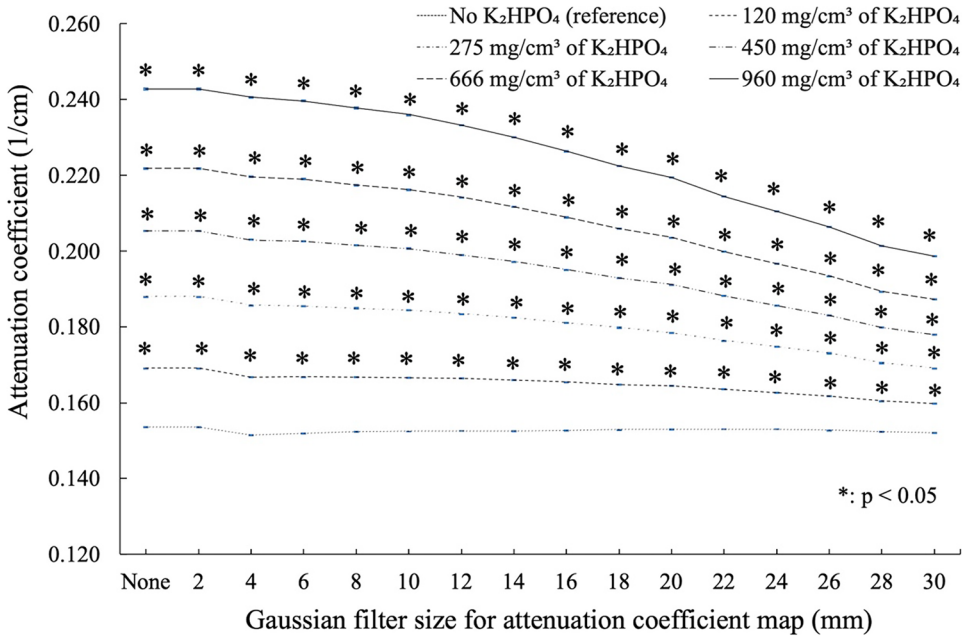

Fig. 3 Attenuation coefficients for each K_2HPO_4 concentration as a function of Gaussian filter size. Attenuation coefficient values were highest for the higher K_2HPO_4 concentration and Gaussian filter sizes of 0–2 mm. Attenuation coefficients were significantly higher for rods at every K_2HPO_4 concentration than for rods without K_2HPO_4 solution at all Gaussian filter sizes ($p < 0.05$). Error bars indicate interquartile range (blue line)

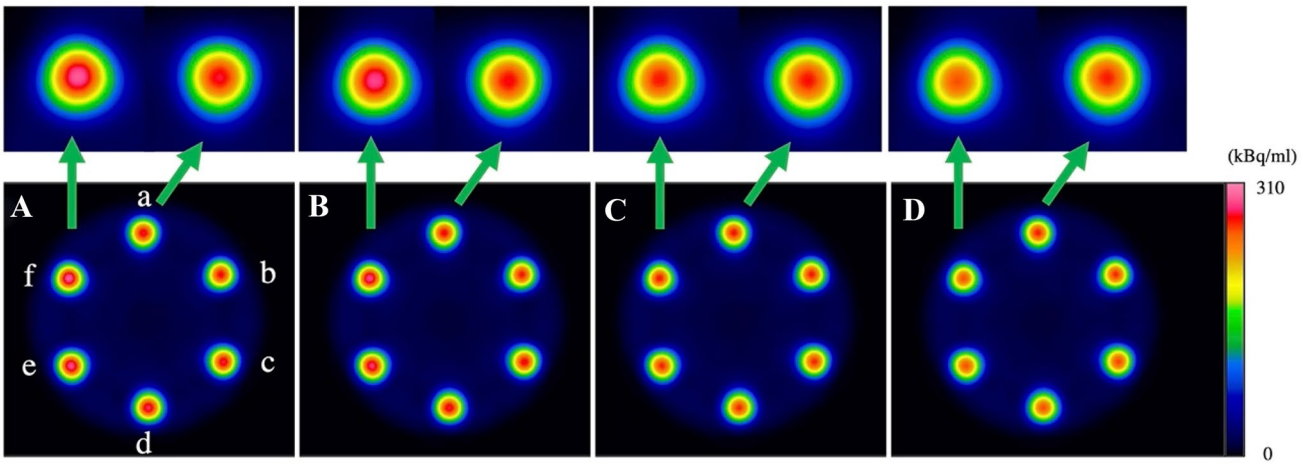

Fig. 4 Attenuation-corrected SPECT images of the phantom using CTAC maps smoothed with no filter (**A**) and Gaussian filter sizes of 10 mm (**B**), 20 mm (**C**), and 30 mm (**D**). Rod (a) was filled with water, and rods (b–e) were filled with K_2HPO_4 solution of concentrations 120 (b), 275 (c), 450 (d), 666 (e), and 960 (f) mg/cm^3 to simulate different bone densities. For small Gaussian filter sizes, the radioactivity concentration increased with increasing K_2HPO_4 concentration

observed at the center of the rod. At higher concentrations of K_2HPO_4, the radioactivity concentration in the center of the rod tended to increase as the Gaussian filter size was reduced.

Discussion

The present study investigated the effect of Gaussian filter size on quantitative bone SPECT/CT assessment using a phantom containing various K_2HPO_4 solutions simulating bone densities. When the Gaussian filter size was set below 14–16 mm, the radioactivity concentration was significantly overestimated in K_2HPO_4 solution concentrations of 666–960 mg/cm^3 (i.e., regions representing high bone density) compared to the region of water without K_2HPO_4 solution. With a Gaussian filter size of 18–22 mm, the difference in radioactivity concentration between the rod of water without K_2HPO_4 solution and the five rods with different concentrations of K_2HPO_4 solution was minimal, with a mean difference within 1.0%.

Smoothing of CTAC maps is an image processing step performed in quantitative analysis of SPECT/CT. Because the SPECT and CT images differ in resolution, the

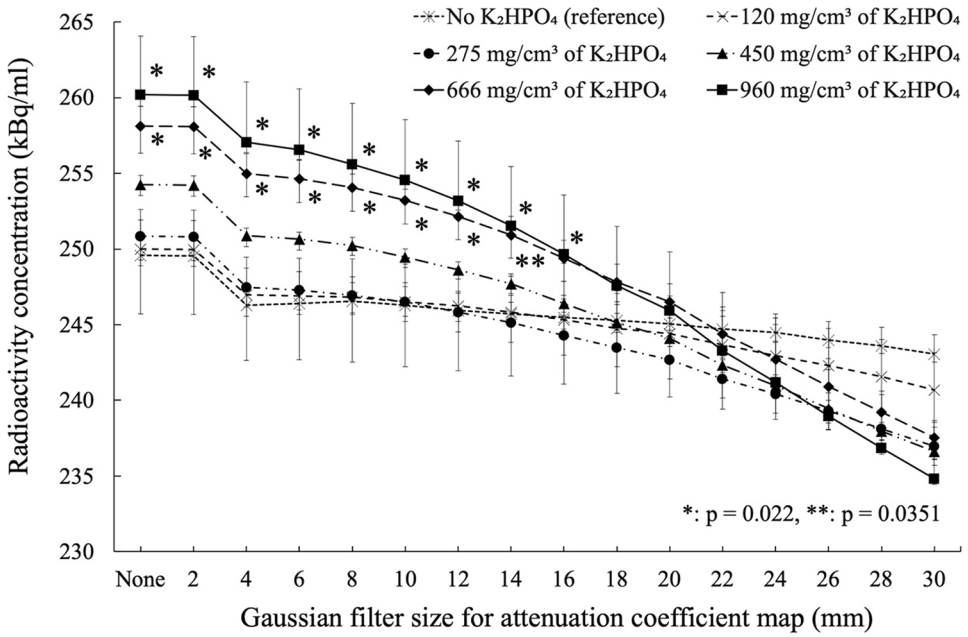

Fig. 5 Radioactivity concentrations of the six rods as a function of Gaussian filter size in the CTAC maps. Radioactivity concentration was significantly higher in rods with K_2HPO_4 concentrations of 666 and 960 mg/cm^3 than in the water-filled rod for Gaussian filter sizes less than 14–16 mm ($p < 0.05$). Error bars indicate interquartile range

boundaries of tissues that have different attenuations in the two images are prone to the artifact. To reduce this effect, the CTAC maps are usually smoothed using a Gaussian filter [11, 12]. The size of the Gaussian filter can affect both image quality and quantitative evaluation of the SPECT image. The default Gaussian smoothing filter size in the SPECT/CT system used in this study is 9 × 9 × 13 mm, but there is currently a lack of evidence on the optimization of the filter size. Optimizing Gaussian filter size is considered important to ensure the quality of SPECT images and the accuracy of SPECT quantitative evaluation. This is the first report to evaluate the effect of the size of the Gaussian filter used for smoothing the CTAC map in SPECT quantitative evaluation. The results of this study can provide important insights for optimizing image reconstruction parameters in performing SPECT quantitative assessment.

CTAC is an essential step in quantitative SPECT/CT evaluation. There are three major processes in performing CTAC. First, the CT matrix size is downsampled to the same format as that used for the reconstructed SPECT data. Second, Hounsfield units (HU) obtained with low energy CT (< 70 keV) are converted to attenuation coefficients corresponding to the radionuclide used in SPECT. In regions of bone, X-ray photons are predominantly absorbed by the photoelectric effect according to differences in the energy and nature of the energy spectra, whereas gamma photons interact with matter principally by the Compton scattering effect. The bone may cause artefactually high attenuation coefficients and overestimation of radioactivity concentration in SPECT. In essence, these differences mean that a simple scaling from HU to an appropriate attenuation factor is not possible. Some studies have demonstrated that conversion from HU to attenuation coefficients demonstrates a bilinear nature [11, 20]. The bilinear model uses one linear attenuation coefficient conversion ratio for air- and-water rich tissue ($-1000 \leq HU \leq 0$) and another for water- and-bone rich tissue ($HU \geq 0$, CT energy dependent) on SPECT imaging to create the CTAC maps [21, 22]. Third, the CTAC maps are smoothed by a Gaussian filter to reduce artifact that occurs at boundaries between differently attenuating tissue due to the different resolutions of SPECT and CT images [11, 12]. In the present study, we investigated the parameter of Gaussian filter size, which must be set in these CTAC processes.

Quantitative evaluation of bone SPECT images provides useful clinical information. According to a recent study of 70 breast cancer patients with bone metastases who underwent bone scintigraphy with ^{99m}Tc-hydroxymethylene diphosphonate (^{99m}Tc-HDP), quantitative SPECT evaluation was useful for differentiating bone metastases from bone degenerative changes, with high diagnostic accuracy (sensitivity 91.5% and specificity 93.3%) when SUV_{max} of 16.6 was used as the cutoff [6]. A quantitative SPECT evaluation in 60 prostate cancer patients treated with ^{223}Ra reported that the group with a higher bone accumulation of ^{99m}Tc-DPD before treatment had a worse prognosis than the group with lower bone accumulation [23]. In these previous studies, CTAC was performed to generate SPECT images for quantitative

Fig. 7 Line profile curves of SPECT images with CTAC map without Gaussian filter (**A**). Line profiles on each rod (**B**–**E**) for CTAC maps with Gaussian filter sizes of 10, 20, and 30 mm

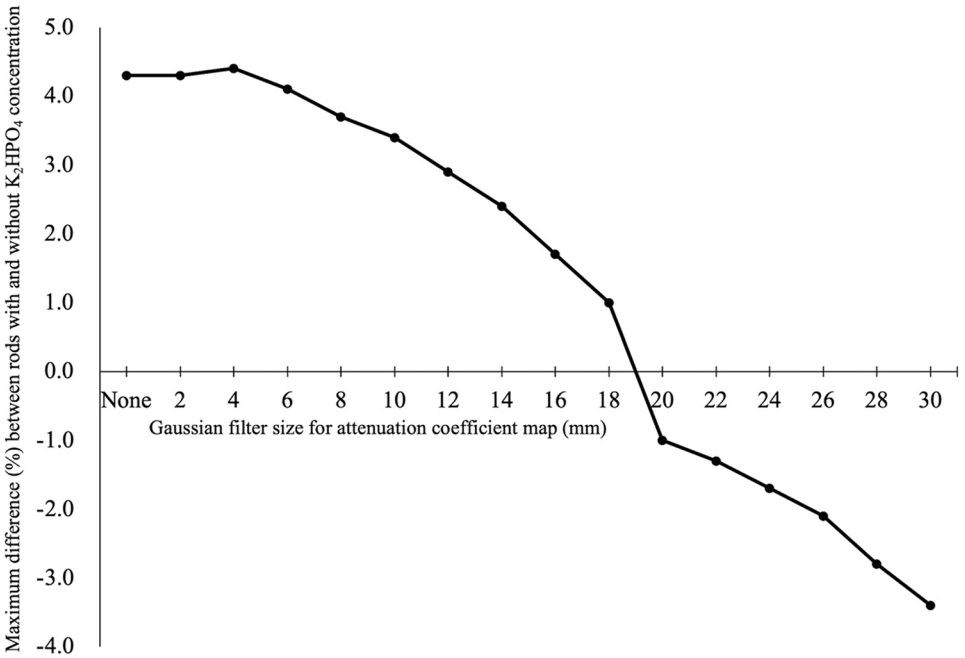

Fig. 6 Maximum difference (%) between rods with and without K_2HPO_4 concentration as a function of Gaussian filter size in the CTAC maps. Maximum difference (%) between rods with and without K_2HPO_4 concentration as a function of Gaussian filter size in the CTAC maps. The maximum difference was observed in the rods with K_2HPO_4 concentrations of 960 mg/cm^3 when the Gaussian filter size was 0–16 mm and 26–30 mm. The maximum differences when Gaussian filter sizes of 18 mm and 20–24 mm were observed in the rods with 666 mg/cm^3 and 275 mg/cm^3, respectively

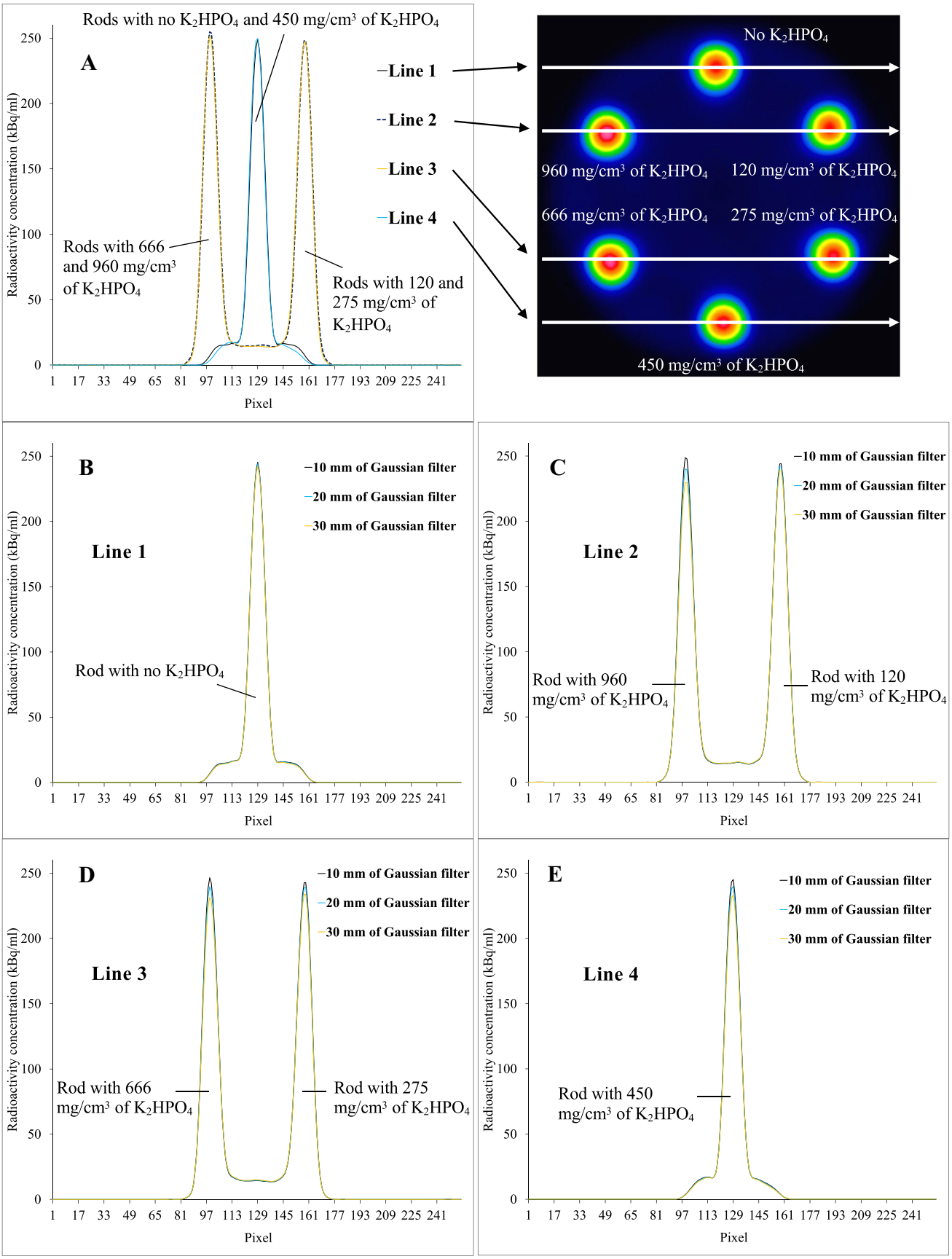
A
Rods with no K_2HPO_4 and 450 mg/cm³ of K_2HPO_4
Line 1
Line 2
Line 3
Line 4
Rods with 666 and 960 mg/cm³ of K_2HPO_4
Rods with 120 and 275 mg/cm³ of K_2HPO_4
No K_2HPO_4
960 mg/cm³ of K_2HPO_4
120 mg/cm³ of K_2HPO_4
666 mg/cm³ of K_2HPO_4
275 mg/cm³ of K_2HPO_4
450 mg/cm³ of K_2HPO_4
Radioactivity concentration (kBq/ml)
Pixel
B
Line 1
Rod with no K_2HPO_4
C
Line 2
Rod with 960 mg/cm³ of K_2HPO_4
Rod with 120 mg/cm³ of K_2HPO_4
D
Line 3
Rod with 666 mg/cm³ of K_2HPO_4
Rod with 275 mg/cm³ of K_2HPO_4
E
Line 4
Rod with 450 mg/cm³ of K_2HPO_4
10 mm of Gaussian filter
20 mm of Gaussian filter
30 mm of Gaussian filter

analysis. However, few previous studies have mentioned the size of the Gaussian filter used in CTAC. The results of the present study suggest that the size of the Gaussian filter in CTAC affects the accuracy of the quantitative evaluation of bone SPECT. Therefore, it is important to optimize and unify the Gaussian filter size to enable the greater utilization of SPECT quantitative evaluation in clinical practice in the future. The present study provides fundamental data that are considered important for the optimization of Gaussian filters used in the quantitative assessment of bone SPECT images.

The measured radioactivity concentration of each cylinder in this study was approximately 20% higher than the true radioactivity concentration (207 kBq/ml). The main reason for this difference can be attributed to the fact that the "maximum value" of the radioactivity concentration in the ROI located in each cylinder was used for the analysis.

The present study has some limitations. First, experiments were performed only at a CT tube voltage of 120 kVp. The tube voltage depends on the attenuation coefficient and may affect the quantitative accuracy of SPECT. Second, this study only evaluates objects of diameter 30 mm, which is a size considered to be minimally affected by partial volume effects. In the future, the influence of the size of the Gaussian filter on SPECT quantitative evaluation in smaller lesion sizes (diameter < 3 cm) should be studied. Third, this study was designed with the assumption that rods of various bone concentrations would all have the same measured activity. However, since each rod has a different material density and some self-attenuation occurs as the photons leave the rod, the activities may not be strictly equal, and no consideration was given to this effect. In order to remove this effect from the evaluation, other methods such as Monte Carlo simulations would need to be performed. Forth, the quantitative accuracy of radionuclides other than ^{99m}Tc used in SPECT has not been assessed.

Conclusions

In the quantitative assessment of bone tissue with SPECT/CT, a Gaussian filter size of 14–16 mm or less results in an overestimation of the radioactivity concentration in the regions of high bone densities. In the bone SPECT quantitative assessment, the Gaussian filter size with the least effect on bone density was 18–22 mm.

Author Contributions All authors contributed to the conception and design of this study. Material preparation, data collection, and analysis were performed by Yoya Tomita and Kengo Hashizume. The first draft of the manuscript was written by Yoya Tomita, and Yasutaka Ichikawa edited the manuscript. All authors read and approved the final manuscript.

Data Availability The datasets generated and/or analyzed during the current study are available from the corresponding author on reasonable request.

Declarations

Ethics Approval This study is a phantom experiment. Ethical approval is not required for this study in accordance with the regulations of the Ethical Review Committee for Medical Research of Mie University Hospital.

Conflict of Interest The authors declare no competing interests.

References

1. Palmedo H, Marx C, Ebert A, Kreft B, Ko Y, Türler A, et al. Whole-body SPECT/CT for bone scintigraphy: diagnostic value and effect on patient management in oncological patients. Eur J Nucl Med Mol Imaging. Jan 2014;41(1):59-67.
2. Utsunomiya D, Shiraishi S, Imuta M, Tomiguchi S, Kawanaka K, Morishita S, et al. Added value of SPECT/CT fusion in assessing suspected bone metastasis: comparison with scintigraphy alone and nonfused scintigraphy and CT. Radiology. Jan 2006;238(1):264-271.
3. Gnanasegaran G, Ballinger JR. Molecular imaging agents for SPECT (and SPECT/CT). Eur J Nucl Med Mol Imaging. May 2014;41 Suppl 1:S26-35.
4. Hashizume K, Ichikawa Y, Tomita Y, Sakuma H. Impact of CT tube-voltage and bone density on the quantitative assessment of tracer uptake in Tc-99m bone SPECT/CT: A phantom study. Phys Med. Dec 2022;104:18-22.
5. Mariani G, Bruselli L, Kuwert T, Kim EE, Flotats A, Israel O, et al. A review on the clinical uses of SPECT/CT. Eur J Nucl Med Mol Imaging. Oct 2010;37(10):1959-1985.
6. Gherghe M, Mutuleanu MD, Stanciu AE, Irimescu I, Lazar A, Bacinschi X, et al. Quantitative Analysis of SPECT-CT Data in Metastatic Breast Cancer Patients-The Clinical Significance. Cancers (Basel). Jan 6 2022;14(2).
7. Qi N, Meng Q, You Z, Chen H, Shou Y, Zhao J. Standardized uptake values of (99m)Tc-MDP in normal vertebrae assessed using quantitative SPECT/CT for differentiation diagnosis of benign and malignant bone lesions. BMC Med Imaging. Feb 27 2021;21(1):39.
8. Tabotta F, Jreige M, Schaefer N, Becce F, Prior JO, Nicod Lalonde M. Quantitative bone SPECT/CT: high specificity for identification of prostate cancer bone metastases. BMC Musculoskelet Disord. Dec 26 2019;20(1):619.
9. Zhang Y, Li B, Yu H, Song J, Zhou Y, Shi H. The value of skeletal standardized uptake values obtained by quantitative single-photon emission computed tomography-computed tomography in differential diagnosis of bone metastases. Nucl Med Commun. Jan 2021;42(1):63-67.
10. Beck M, Sanders JC, Ritt P, Reinfelder J, Kuwert T. Longitudinal analysis of bone metabolism using SPECT/CT and (99m)Tc-diphosphono-propanedicarboxylic acid: comparison of visual and quantitative analysis. EJNMMI Res. Dec 2016;6(1):60.
11. Bailey DL, Willowson KP. Quantitative SPECT/CT: SPECT joins PET as a quantitative imaging modality. Eur J Nucl Med Mol Imaging. May 2014;41 Suppl 1:S17-25.
12. Ljungberg M, Pretorius PH. SPECT/CT: an update on technological developments and clinical applications. Br J Radiol. Jan 2018;91(1081):20160402.

13. Ay MR, Shirmohammad M, Sarkar S, Rahmim A, Zaidi H. Comparative assessment of energy-mapping approaches in CT-based attenuation correction for PET. Mol Imaging Biol. Feb 2011;13(1):187-198.
14. Ghoncheh Z, Kaviani H, Ghadiri Harvani H, Goodarzipoor D, Shamshiri AR, Shams P. Assessment of the Capability of Bone Density Contrast Dissociation in Cone Beam Computed Tomography Compared to Digital Periapical Radiography by Using a Phantom. J Dent (Shiraz). Sep 2019;20(3):203-209.
15. Oliveira ML, Tosoni GM, Lindsey DH, Mendoza K, Tetradis S, Mallya SM. Influence of anatomical location on CT numbers in cone beam computed tomography. Oral Surg Oral Med Oral Pathol Oral Radiol. Apr 2013;115(4):558-564.
16. Reza Ay M, Zaidi H. Computed tomography-based attenuation correction in neurological positron emission tomography: evaluation of the effect of the X-ray tube voltage on quantitative analysis. Nucl Med Commun. Apr 2006;27(4):339-346.
17. Lee S, Chung CK, Oh SH, Park SB. Correlation between Bone Mineral Density Measured by Dual-Energy X-Ray Absorptiometry and Hounsfield Units Measured by Diagnostic CT in Lumbar Spine. J Korean Neurosurg Soc. Nov 2013;54(5):384-389.
18. Schreiber JJ, Anderson PA, Rosas HG, Buchholz AL, Au AG. Hounsfield units for assessing bone mineral density and strength: a tool for osteoporosis management. J Bone Joint Surg Am. Jun 1 2011;93(11):1057-1063.
19. Ulano A, Bredella MA, Burke P, Chebib I, Simeone FJ, Huang AJ, et al. Distinguishing Untreated Osteoblastic Metastases From Enostoses Using CT Attenuation Measurements. AJR American journal of roentgenology. Aug 2016;207(2):362-368.
20. Ritt P, Sanders J, Kuwert T. SPECT/CT technology. Clin Transl Imaging. 2014;2:445–457.
21. Bocher M, Balan A, Krausz Y, Shrem Y, Lonn A, Wilk M, et al. Gamma camera-mounted anatomical X-ray tomography: technology, system characteristics and first images. Eur J Nucl Med. Jun 2000;27(6):619-627.
22. Fricke E, Fricke H, Weise R, Kammeier A, Hagedorn R, Lotz N, et al. Attenuation correction of myocardial SPECT perfusion images with low-dose CT: evaluation of the method by comparison with perfusion PET. Journal of nuclear medicine : official publication, Society of Nuclear Medicine. May 2005;46(5):736-744.
23. Dittmann H, Kaltenbach S, Weissinger M, Fiz F, Martus P, Pritzkow M, et al. The Prognostic Value of Quantitative Bone SPECT/CT Before (223)Ra Treatment in Metastatic Castration-Resistant Prostate Cancer. Journal of nuclear medicine : official publication, Society of Nuclear Medicine. Jan 2021;62(1):48-54.